Taibah University

Journal of Taibah University Medical Sciences

www.sciencedirect.com

Original Article

Obstructing *Salmonella typhi*'s virulence in eukaryotic cells through design of its SipB protein antagonists

John P. Ameji, M.Sc [a],[*], Adamu Uzairu, PhD [b], Gideon A. Shallangwa, PhD [b] and Sani Uba, PhD [b]

[a] *Department of Chemistry, Federal University Lokoja, Lokoja, Nigeria*
[b] *Department of Chemistry, Ahmadu Bello University, Zaria, Kaduna State, Nigeria*

المصممة أنها متوفرة بيولوجيا عن طريق الفم وتظهر سمات حركية دوائية ممتازة.

الاستنتاجات: يمكن أن توفر النتائج في هذا البحث خارطة طريق إيجابية لاكتشاف مضادات حيوية أحدث وأكثر فعالية ضد السالمونيلا التيفية.

الكلمات المفتاحية: السالمونيلا التيفية، حمى التيفوئيد، الحرائك الدوائية.

المخلص

أهداف البحث: حمى التيفوئيد، مرض تسببه السالمونيلا التيفية هي سبب رئيسي للمراضة والوفيات خاصة في الدول النامية. استلزم تطور آليات المقاومة المختلفة للمضادات الحيوية الموجودة البحث عن أدوية مرشحة جديدة. استخدمت هذه الدراسة تقنيات تصميم الأدوية بمساعدة الكمبيوتر لتصميم مضادات حيوية جديدة تعمل عن طريق استهداف "سيب.ب"، وهو بروتين مؤثر للبكتيريا المسؤولة عن إمراضها وحدوثها في الخلية المضيفة حقيقية النواة.

طرق البحث: تم استرداد مجموعة بيانات من 32 جزيء نشطا بيولوجيا ذات أنشطة مضادة للجراثيم ضد السالمونيلا التيفية من قاعدة بيانات "بوبكيم". تم تحسينها من خلال نهج الدالة الوظيفية للكثافة باستخدام برنامج "سبارتان 14" وخضعت كذلك لنمذجة علاقة الهيكل بالنشاط الكمي. باستخدام برنامج "بيوفيا- ستوديو". يكشف النموذج الذي تم التحقق منه التأثير المهيمن لوصف "ماتز6.سي" و "إي.3.ب" على الأنشطة المضادة للبكتيريا المرصودة للمركبات. تم استخدام المعلومات من النموذج لتحسين هياكل العملاء المتوقعين المختارين في مجموعة البيانات لتصميم مجموعة فعالة للغاية من نظائرها الجديدة التي تحمل الاسم الرمزي د-1 و د-2 و د-3.

النتائج: القيم المتوقعة هي 1.03 ميكروغرام/مل لـ د-1 ؛ و 0,73 ميكروغرام/ مل لـ د-2 ؛ و 0.30 ميكروغرام/مل لـ د-3. علاوة على ذلك، تكشف دراسات الالتحام الجزيئي على هذه الروابط الجديدة مقابل المواقع النشطة لـ "سيب.ب" عن قيم طاقة ملزمة تبلغ -8.0 و -7.7 و -7.7 كيلو كالوري / مول لـ د-1 و د-2 و د-3، على التوالي. هذه القيم أفضل مقارنة بـ -7.0 كيلو كالوري/مول المسجلة للسيبروفلوكساسين، المضاد الحيوي المرجعي المستخدم هنا لضمان الجودة. أيضا، تظهر تقييمات التشابه الدوائي وتقييمات الحركيات الدوائية للمركبات

ELSEVIER   **Production and hosting by Elsevier**

Abstract

Objective: Typhoid fever, a disease caused by *Salmonella typhi*, is a leading cause of morbidity and mortality, particularly in developing nations. The evolution of resistance mechanisms to existing antibiotics has necessitated a search for newer drug candidates. This study used computer aided drug design techniques to design novel antibiotics that function by antagonizing SipB, an effector protein of the bacterium that is responsible for its pathogenicity and virulence in eukaryotic host cells.

Methods: A data set of 32 bioactive molecules with established antibacterial activity against *S. typhi* was retrieved from the PubChem data base; optimized through a DFT approach in Spartan 14 software; and further subjected to QSAR modeling in BIOVIA- Accelrys Material Studio. The validated model ($R^2 = 0.80$, $R^2_{Adj} = 0.78$, $Q^2_{LOO} = 0.74$, $R^2_{pred} = 0.54$, lack of fit = 0.07) revealed the dominant influence of MATS6c and E3p descriptors on the observed antibacterial activity of the compounds. Information from the model was used to optimize the structures of selected lead compounds in the data set, thus leading to the design of a highly potent set of novel analogues denoted D-1, D-2 and D-3.

Results: The predicted MIC values of D-1, D-2 and D-3 were 1.03, 0.73 and 0.30 µg/mL, respectively. Furthermore, molecular docking studies on these novel ligands against the active sites of SipB revealed binding energy values of −8.0, −7.7 and −7.7 kcal/mol for D-1, D-2 and D-3, respectively. These values were better than the −7.0 kcal/mol recorded for ciprofloxacin, the reference antibiotic used herein for quality assurance. In addition, drug-likeness and ADMET evaluation of the designed compounds revealed that they are orally bioavailable and exhibit excellent pharmacokinetic and toxicological profiles.

Conclusion: The current findings may provide a roadmap for the discovery of more potent antibiotics against *S. typhi*.

Introduction

Salmonella typhi (*S. typhi*) is a rod-shaped flagellated gram-negative bacterium responsible for typhoid fever. The virulence of this human-specific pathogen arises from its enclosure within a polysaccharide capsule that provides protection by deceiving the host immune system.[1] Typhoid fever poses a major health challenge, particularly in developing nations, and causes an estimated 700,000 deaths per year.[1,2] If newer antibiotics are not discovered to overcome the increasing multidrug resistance in *S. typhi*, the global annual mortality has been predicted to rise to 10 million deaths by the year 2050, thereby resulting in an economic loss of $100 million per year.[1] This infectious disease is transmitted through the fecal-oral route, and it is treated with antibiotics such as chloramphenicol, ampicillin and trimethoprim-sulfamethoxazole, as well as fluoroquinolones and third-generation cephalosporin. Emerging multi-drug resistant strains of this bacterium have made the treatment of typhoid fever a major challenge.[3]

To save humanity from a situation similar to that in the pre-antibiotic era, the growing incidence of resistance by this organism must be countered by discovery of newer antibiotics in the drug development pipeline. However, the enormous time and resources required for conventional trial and error approaches remain major bottlenecks to drug discovery. This problem could be circumvented by the application of computer aided drug design (CADD) techniques.[4]

Prominent among the CADD techniques is quantitative structure-activity relationship (QSAR) modeling, which uses Hansch's approach to link the molecular descriptors of a set of compounds to their biological properties in the form of a regression equation, such as equation (1).[5] Information derived from the QSAR model helps optimize the potency,

selectivity, pharmacokinetics and toxicity of lead compounds through modification of its pharmacophore.[6]

$$Y = \alpha x + \beta y + \gamma z \cdots + c \tag{1}$$

where Y is the biological activity of interest; x, y and z are the descriptors; α, β and γ are the numerical coefficients; and c is the constant of the regression equation.

Another in silico technique widely used in modern drug research is molecular docking, an approach that predicts the binding modes and affinities of ligands (small molecules) with their receptors (macromolecules). This technique uses a markedly enlarged equation encompassing entropic parameters in the molecular mechanics models. The strength of the binding between the ligands and receptors is measured as the free energy of binding (ΔG). The energy variables that constitute the ΔG scoring function are shown in equation (2).

$$\Delta G = \Delta G_V + \beta 1 \Delta G_H + \beta 2 \Delta G_E + \beta 3 \Delta G_C + \beta 4 \Delta G_T + \beta 5 \Delta G_S + \beta 6 T \Delta S_T \tag{2}$$

where ΔG_V, $\beta 1 \Delta G_H$, $\beta 2 \Delta G_E$, $\beta 3 \Delta G_C$, $\beta 4 \Delta G_T$ and $\beta 5 \Delta G_S$ are free energy terms for van der Waals, hydrogen bonding, electrostatic, conformational strain penalty, restriction of internal rotors, global rotation, translation and the desolvation penalty associated with binding, respectively. The added entropic term ΔST is based on the rotatable torsion count, which is constant when poses of the same ligand are considered. Likewise, T is the temperature in Kelvin, and $\beta 1-\beta 6$ are ligand and biomolecule parameter coefficients.[7] The docking of the ligands to active sites of the receptor in Autodock Vina enables allocation of scores to the molecules with a scoring algorithm.

S. typhi, after being ingested through the fecal-oral route, adheres to epithelial lining of the ileum and colon and causes gastrointestinal infections.[8] However, owing to the harsh conditions of the extracellular milieu, including factors such as low pH, shear stress due to mucosal secretions or blood, and host defense mechanisms, this pathogen has evolved molecular strategies to actively induce its entry into target cells, thus enabling its replication and dissemination to other host tissues. The pathogenicity island-1 (SPI-1) type III secretion system (T3SS) is a crucial pathogenic element of *S. typhi* that enables the translocation of virulence proteins, known as effectors, via a flagellum-like injectisome from the cytoplasm of the bacterial cell across the inner and outer membrane leaflets to the cytoplasm of a eukaryotic host cell.[9,10] The virulence of *S. typhi* is dependent on the expression of these proteins in eukaryotic host cells.[11] SipB, an effector protein that enhances the virulence of this bacterium, is an enzyme with major roles, including the activation of caspase-1 and subsequent induction of inflammation and autophagy in macrophages, and the promotion of osmo-tolerance.[12,13] In addition, research has shown that the suppression of SipB in *S. typhi* significantly decreases its adherence, invasion and virulence.[14] Thus, the design of bioactive molecules that disrupt the activity of this enzyme is a rational drug design strategy.

We conducted a literature search to review recent in silico studies on inhibitors of SipB in *S. typhi*. Notably, Verma

Table 1: Structures, PubChem CIDs and biological activities of the data set.

S. No	Structure	MIC (μg/ml)	S. No	Structure	MIC (μg/ml)
*1	PubChem CID: 136498831	25	18	PubChem CID 136498787	3.1
2	PubChem CID 136498833	12.5	19	PubChem CID 136498789	3.1
3	PubChem CID 136498835	50	*20	PubChem CID 136498791	3.1
4	PubChem CID 136498837	6.2	21	PubChem CID 136498793	1.56
5	PubChem CID 136498839	3.1	22	PubChem CID 136498795	25
6	PubChem CID 136498841	3.1	*L23	PubChem CID 136498797	25
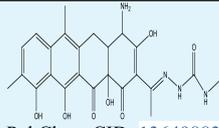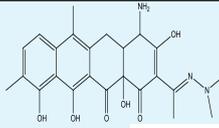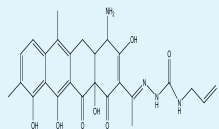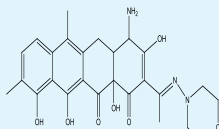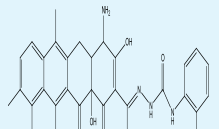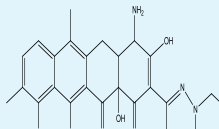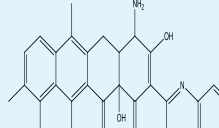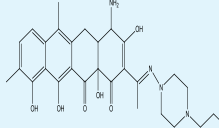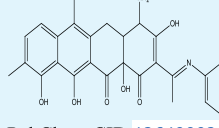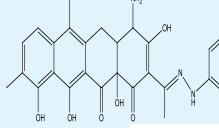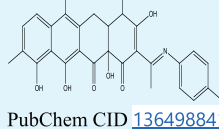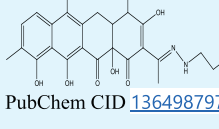
et al.[15] have performed molecular docking studies on several natural products against the cell invasion protein SipB from *S. typhi*. They have discovered 15 molecules with very good docking scores against the target protein via hydrophobic and hydrogen bond interactions. The pharmacokinetic profiles of the compounds revealed that all 15 natural molecules display good drug likeness and do not violate the Lipinski, Ghose, Veber, Egan and Muegge rules.

The goal of this study was to use QSAR and molecular docking techniques to design highly potent ligands that act as antagonists of the SipB enzyme. The pharmacokinetic and toxicological profiles of the novel compounds were determined to ascertain their fates in the biological system. The potency of the novel ligands was compared with that of an approved antibiotic (ciprofloxacin) as a quality control and assurance strategy.

Materials and Methods

Collection of data and molecular optimization

A data set of 32 chelocardin derivatives, numbered 1–32, and their biological activity against *S. typhi*, was retrieved from the PubChem online data source (https://pubchem. ncbi.nlm.nih.gov/). Their bioactivity, expressed as MIC, was transformed to logarithmic form as pMIC (pMIC = −log MIC) to minimize data dispersion. The pMIC, chemical structures and PubChem identification numbers (PubChem CID) of these compounds are presented in Table 1. The 2D structures of the studied molecules drawn in ChemDraw Ultra 12.0 were converted to 3D structures in Spartan 14 version 1.1.4 software from Wavefunction Inc. Geometry optimization of the molecules was performed by

| 7 | | 12.5 | 24 | | 25 |

PubChem CID 136498823   PubChem CID 136498799

| 8 | | 25 | *25 | | 6.2 |

PubChem CID 136498825   PubChem CID 136498801

| 9 | | 25 | 26 | | 1.5 |

PubChem CID 136498827   PubChem CID 167442

| 10 | | 6.2 | 27 | | 12.5 |

PubChem CID 136498829   PubChem CID 136498805

| 11 | | 12.5 | *28 | | 12.5 |

PubChem CID 136498821   PubChem CID 136498807

| 12 | | 3.1 | *29 | | 25 |

PubChem CID 136498843   PubChem CID 136498809
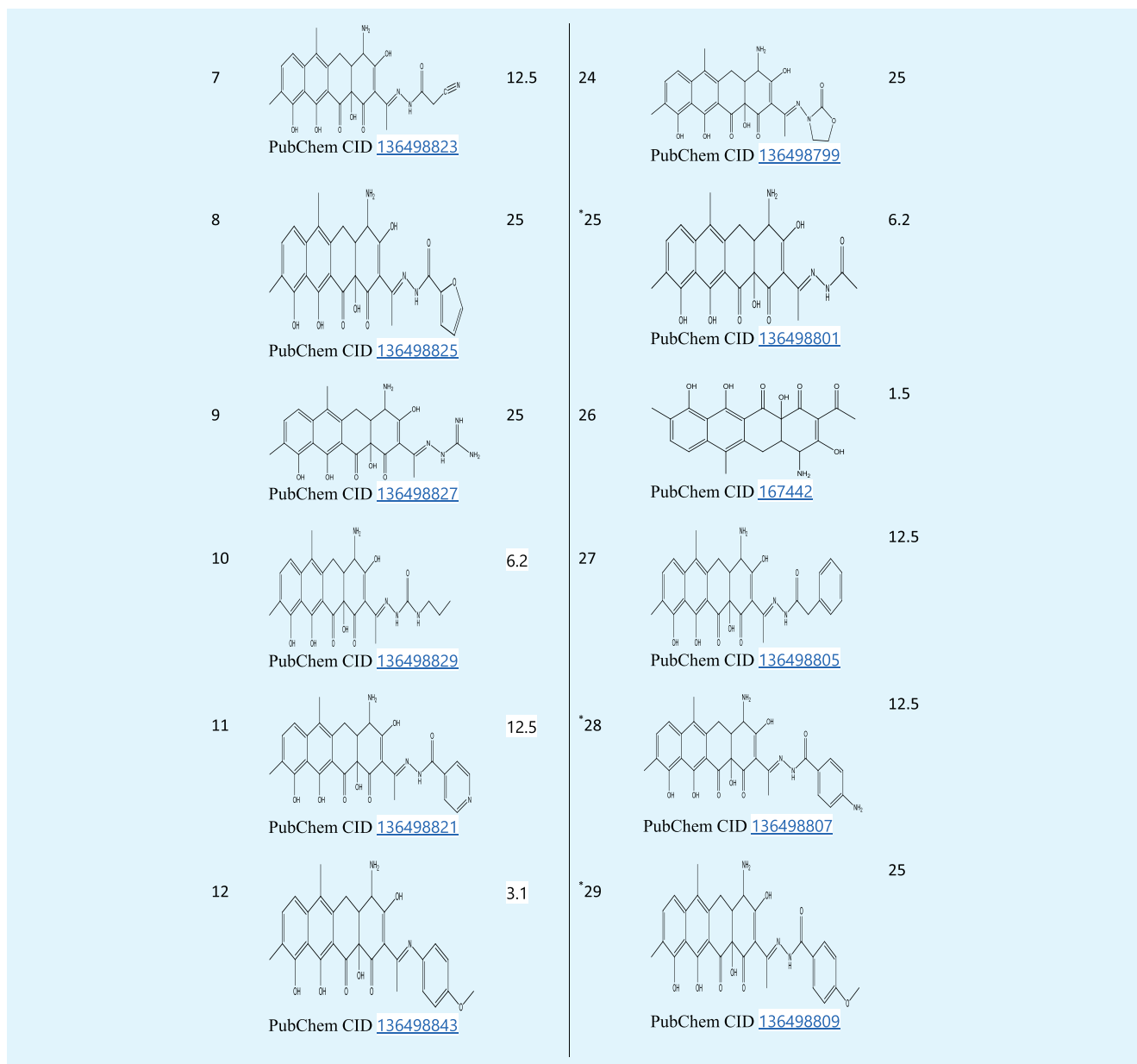
using a density functional theory (DFT/B3LYP) approach and the 6-31G* basis set. The molecular descriptors of the optimized 3D structures were subsequently computed with the PaDEL descriptor tool kit.[16]

QSAR model building and validation

The data set of molecules was split 70% into a training set for model building and 30% into a test set for external validation of the model with the DatasetDivisionGUI V2.1 tool from the DTC laboratory. Redundant descriptors were removed from the computed descriptor pool with the V-WSP data pretreatment tool 1.2v.[17,18] Model building was performed with the Genetic Function Approximation (GFA) method in Material Studio Software (version 8.0) from BIOVIA-Accelrys by setting the minimum and

maximum descriptor numbers in the regression model to 3 and 5, respectively. The mutation probability was set to 0.1, and the smoothing parameter was set to 0.5. In addition, population and generation were set to 1,000 and 5,000, respectively. A unique feature of the GFA technique is its ability to generate a population of models rather than a single model. GFA develops excellent models because its algorithm selects basis functions genetically and ranks the models according to their "lack of fit" scores.[19,20] The best model was validated with the following parameters; least squares fit (R^2), cross validated R-squared (Q^2_{LOO}), adjusted R-squared ($R^2_{Adj.}$) and correlation coefficient for an external prediction set (R^2_{pred}).

Applicability domain definition

The applicability domain (AD) refers to the chemical space of molecules within the jurisdiction of a QSAR model.

13   6.2
PubChem CID 136498845

14   3.1
PubChem CID 136498847

*L15   1.5
PubChem CID 136498849

16   1.5
PubChem CID 136498851

*17   1.5
PubChem CID 136498855

25
*30
PubChem CID 136498811

100
*31
PubChem CID 136498813

32   6.2
PubChem CID 136498813

12.5
*33
PubChem CID 136498803

34   1.5
PubChem CID 136498857
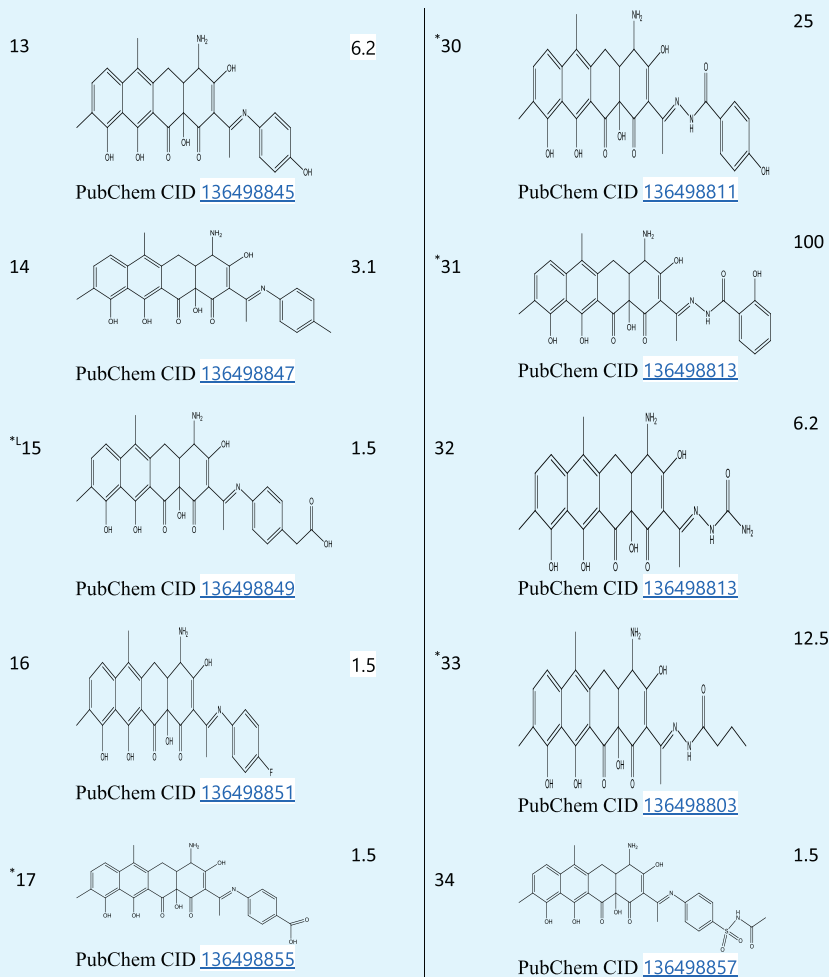
*Test set; ᴸstatistical outlier.

A defined AD helps mitigate possible uncertainties in the prediction of a molecule according to its similarity to the training set of molecules. The AD of our model was defined with the standardization approach in an AD executable jar file in DTC laboratory.[21]

Design

Compounds 16, 21, 26 and 34 were selected as lead compounds (template molecules) for designing new analogues because they fell within the AD of the model and displayed the best antibacterial activity against *S. typhi*. The generated QSAR model revealed that MATS6c, a descriptor of charges plays a major role in the observed antibacterial activity of the compounds. Consequently, the antibacterial activity of the compounds was expected to be enhanced by increasing the number of functional groups possessing electric charges. Guided by this information, we optimized the structures of the lead compounds through the attachment of polar functional groups, such as $-NO_2$, and carbonyl groups as well as halogens. The MIC values of the different analogues generated were then evaluated with equation (3) and the optimum QSAR model, and the best were selected as the novel analogues.

Ligand-protein preparation and docking studies

The newly designed ligands were optimized with the protocols described in Section 2.1 and saved in PDB file format in the Spartan 14 software interface. The X-ray structure of the SipB protein target (PDB code: 3TUL) was retrieved from www.rcsb.org. The target was imported into Discovery Studio Visualizer version 16.1.0.15350, where water molecules and heteroatoms were removed. The prepared protein was further imported into the AutoDock Vina interface, where missing atoms were verified and repaired, partial atomic charges were assigned, and all necessary valency tests and H-atom additions were performed. The PDB files of the novel ligands were docked into the active domain of the SipB enzyme with the AutoDock vina PyRx docking and virtual screening program. As a quality assurance measure, we docked ciprofloxacin, a quinolone based antibiotic currently in use for the treatment of *S. typhi* infections, with the target protein. The same docking procedures were used for the novel analogues, and their binding affinities were compared.[22]

Drug-likeness evaluation and ADME/T prediction

Drug likeness is a measure of the oral bioavailability of a therapeutic compound. This important parameter was

Table 2: Standard QSAR validation parameters versus model parameters.

S/n	Parameter	Threshold	Model value	Statement
1.	Square of coefficient of determination (R^2)	≥ 0.6	0.80	Excellent
2.	Adjusted R-squared ($R^2_{Adj.}$)	≥ 0.6	0.78	Stable
3.	Cross validated R-squared (Q^2_{LOO})	≥ 0.5	0.74	Reliable
4.	Predictive R-squared (R^2_{pred})	≥ 0.5	0.54	Robust
5.	$R^2 - Q^2_{LOO}$	≤ 0.3	0.06	Stable
6.	Lack of fit (LOF) score	Low	0.07	Stable

evaluated for all novel ligands on the basis of Lipinski's rule. According to this rule, a drug must not violate more than one of the following considerations to be orally bioavailable: molecular weight <500 g/mol, number of hydrogen bond donors <5, octanol/water partition coefficient (log P) < 5 and number of hydrogen bond acceptors <10.[23] The physicochemical properties defining the drug likeness of the molecules were calculated with the SwissADME (www.swissadme.ch/) online tool and DataWarrior software.

Likewise, the fate and distribution of the designed drug-like compounds in the biological system, with particular reference to their absorption (A), distribution (D), metabolism (M) and excretion (E), known as pharmacokinetic[24] and potential toxicity (T), were evaluated with the Swiss ADME server (http://www.swissadme.ch/index.php) and DataWarrior software, which predicts mutagenicity, reproductive effects and the tendency of a compound to cause irritation.

Results

QSAR model and authentication

The GFA derived QSAR regression model for estimating the inhibitory activity of the studied compounds against *S. typhi* is presented in Equation (3). Tables 2 and 3 present the validation parameters and definitions of the descriptors in the model, respectively. The correlation matrix for the two descriptors in the model is shown in Table 4. Furthermore, the plot of experimental pMIC against predicted pMIC for training and test set molecules is shown in Figures 1 and 2, respectively. Likewise, Figures 3 and 4 present the residual plot of the model and the percentage influences on the experimental antibacterial activity of the compounds, respectively.

$$pMIC = 9.012*MATS6c - 5.2822*E3p + 0.9783 \quad (3)$$

Table 3: Symbols, definitions, and classes of the descriptors in Equation 3.

S/n	Descriptor	Definition	Class
1	MATS6c	Moran autocorrelation - lag 6/weighted by charges	2D
2	E3P	Third component accessibility directional WHIM index/weighted by relative polarizability	3D

Table 4: Correlation matrix of descriptors.

	pMIC	MATS6c	E3p
pMIC	1		
MATS6c	0.7538	1	
E3p	−0.536	−0.0775	1
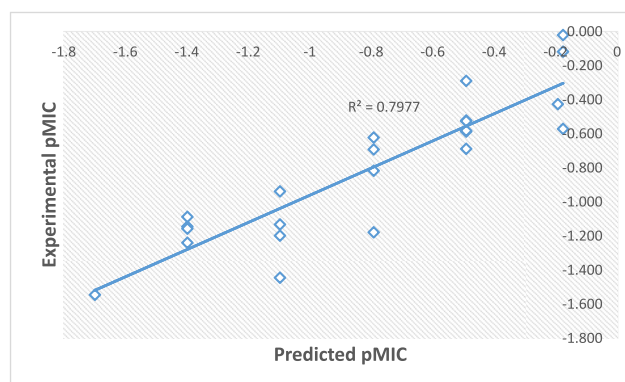
Figure 1: Plot of experimental pMIC verses predicted pMIC (training set).

Novel ligands and their predicted MIC values

The 2D chemical structures of the designed ligands, denoted D-1, D-2 and D-3, and the ciprofloxacin antibiotic used for quality assurance are presented in Figure 5. The novel ligands were geometry optimized, and their
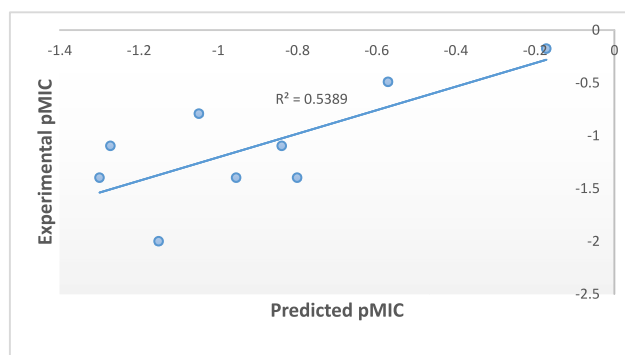
Figure 2: Plot of experimental pMIC against predicted pMIC (test set).
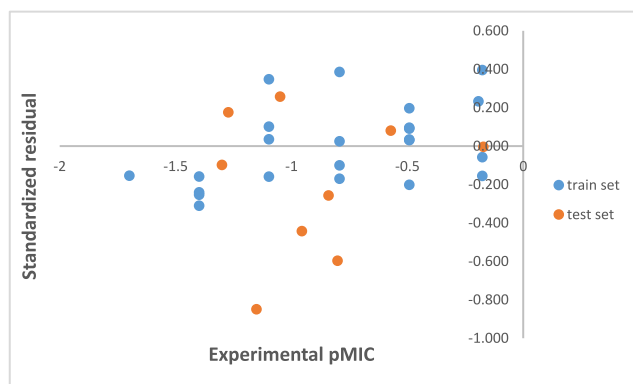
Figure 3: Residual Plot of the Model.

descriptors were calculated with the methods described in Section 2.1. The dominant descriptors of the antibacterial activity of the compounds, as revealed by the QSAR model in Equation (3), were determined, and their MIC values were computed with the equation. The results are presented in Table 5.

Molecular docking simulation studies on the designed compounds

The binding affinities (ΔG) of the novel ligands and ciprofloxacin antibiotic with the SipB protein target are presented in Table 6, and their 2D interaction diagrams are shown in Figure 6.

Drug-likeness and ADMET data

The major physicochemical properties and in silico assays of the novel bioactive compounds needed for full evaluation of their oral bioavailability and ADMET profiles are presented in Table 7.

Discussion

QSAR model

Equation (3) shows the QSAR model developed for predicting the inhibitory activity of the studied compounds
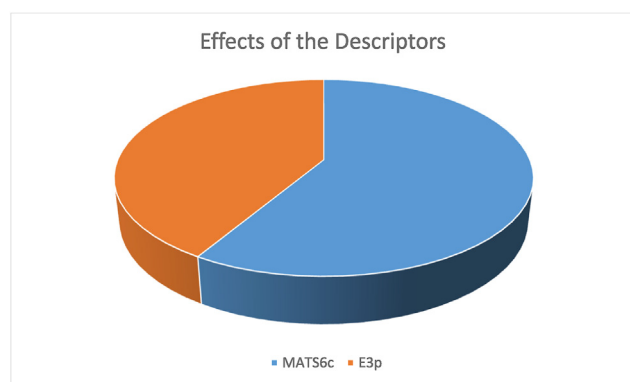
Figure 4: Influence of the descriptors in the Model on antibacterial properties.

against *S. typhi*. The stability, robustness and quality of the model were assessed by comparison of the validation parameters with standard values for general QSAR models. The results (Table 2) indicated that the model was sound and reliable, because all parameters were within the standard thresholds.[25,26] Likewise, the high linearity of the plot of the experimental versus predicted pMIC values for the training set compounds (Figure 1) further confirmed the internal stability and soundness of the model. In addition, the ability of the model to predict the antibacterial activity of external sets of molecules within the applicability domain was assessed, on the basis of external validation through the plot of experimental versus predicted pMIC for the test set compounds (Figure 2). The predictive R^2 (R^2_{pred}) value of 0.54 within the recommended threshold for this parameter (Table 2) implied that the model provided a good prediction of the antibacterial activity of new chemicals within its applicability domain. The symbols, definitions and classes of the descriptors in the model are presented in Table 3.

Furthermore, the presence of possible systematic error during the course of the QSAR model building was verified through the plot of standardized residuals against the experimental pMIC values (Figure 3). The propagation of residuals on both sides of the zero line confirmed the absence of systematic error in model development.[27]

Likewise, strong inter-correlations among the descriptors in a QSAR model weaken its statistical power and stability. The correlation matrix presented in Table 4 revealed a very low inter-correlation ($R^2 = -0.0775$) between descriptors, thereby indicating the high statistical strength and soundness of the model.

Significance of the descriptors in the model

The influences of the descriptors in the QSAR model on the observed antibacterial activity of the compounds are presented in Figure 4. Analysis of the graph revealed the predominant influence of MATS6c over E3p. The positive coefficient of MATS6c, a descriptor of charges in a molecule, was positively correlated with the antibacterial activity of the compounds. Thus, for enhanced anti-*S. typhi* activity, polar functional groups, such as nitro and carbonyl functional groups, should be attached to the parent structures. In addition, E3p, a descriptor of the relative polarity of covalent bonds in a molecule, had the least influence on the observed antibacterial activity of the compounds. This descriptor was negatively associated with the antibacterial activity of the compounds, as revealed by its negative correlation with pMIC in the model.

Molecular docking simulation studies

The major antibiotics currently used for the management and treatment of *S. typhi* infections are β-lactam and quinolone based antibiotics. The former act by disrupting penicillin binding protein enzymes, whereas the latter act by binding DNA gyrase and topoisomerase IV in the bacterium. However, given the different resistance mechanisms of *S. typhi* toward these antibiotics, designing bioactive entities targeting other essential enzymes of the bacterium is desirable. One such enzyme is the cell invasion protein SipB,
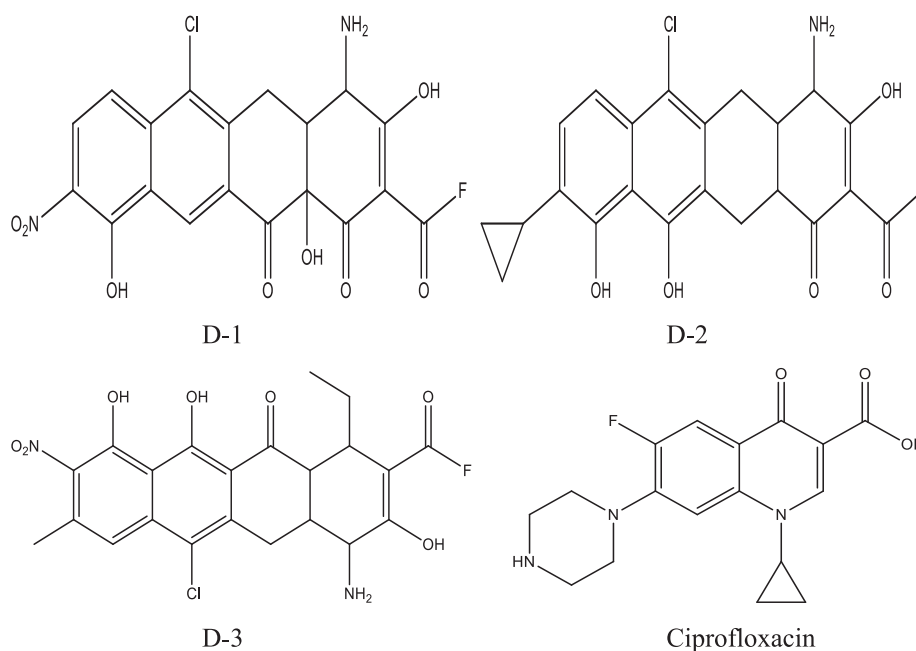
Figure 5: 2D chemical structures of the novel ligands and ciprofloxacin D-1: 4-amino-6-chloro-3, 10, 12a-trihydroxy-9-nitro-1, 12-dioxo-1, 4, 4a, 5, 12, 12a-hexahydrotetracene-2-carbonyl fluoride, D-2: 4-amino-6-chloro-9-cyclopropyl-3, 10, 11-trihydroxy-1-oxo-1, 4, 4a, 5, 12, 12a-hexahydrotetracene-2-carbonyl fluoride, D-3:4-amino-6-chloro-1-ethyl-3, 10, 11-trihydroxy-8-methyl-9-nitro-12-oxo-1, 4, 4a, 5, 12, 12a-hexahydrotetracene-2-carbonyl fluoride.

which plays major roles in invasion and virulence. Here, we performed molecular docking analysis of the designed ligands to examine their binding patterns with SipB protease and compare them with those of the standard ciprofloxacin inhibitor. The newly designed compounds (Figure 5) had a minimum binding energy ranging from −7.7 to −8.4 kcal/mol (Table 6), and the best result was achieved with D-1. All compounds displayed better binding efficacies than the −7.0 kcal/mol recorded for the standard inhibitor ciprofloxacin (Table 6).

Figure 6 presents the various interactions of the designed ligands and ciprofloxacin with the active sites of the protease SipB. Ligand D-1, with a docking score of −8.1 kcal/mol, binds the active sites of the protease via hydrophobic interactions with residues THR 94, THR 206 and LEU 89 in pi-cation, Van der Waals and alkyl type interactions, respectively. These associations are stabilized by five conventional hydrogen bonds with THR 94, THR 150, THR 206 and LEU 89. In addition, the docking score for ligand D-2 with the protease is −7.7 kcal/mol. The ligand forms two π−π stacked and one π−σ associations with PHE 129, and two conventional hydrogen bonds with the SER 126 and GLU 128 amino acid side chains of the protein target. Furthermore, ligand D-3 forms three alkyl interactions with LEU 89, LEU 92 and LEU 96, and a π−cation interaction with THR 94. These interactions are stabilized by five conventional hydrogen bonds with THR 150 and THR 206 of the target. Ciprofloxacin, the

reference antibiotic used for quality assurance, has a docking score of −7.0 kcal/mol and displays only hydrophobic interactions with PHE 129 (π−π stacked and π alkyl types), TRP 111 (π alkyl type), SER 126 (Van der Waals types) and GLU 128 (carbon−hydrogen type) of the target.

The designed ligands show better binding to the active sites of SipB than ciprofloxacin, owing to the absence of conventional hydrogen bond interactions in the latter. In addition, all designed ligands show different mechanisms of interactions with the protease, except D-2 which displays a slightly similar binding interaction with ciprofloxacin, in that both display π−π stacked interactions with PHE 129 of the protease. In addition, both interact with SER 129 of the target enzyme.

Drug-likeness and ADMET profiles of the designed compounds

The drug likeness of the designed ligands was evaluated with Lipinski's rule, which states that a drug must not violate more than one of the following parameters to be orally bioavailable; molecular weight <500, number of hydrogen bond donors <5, octanol/water partition coefficient (log P) < 5 and number of hydrogen bond acceptors <10. The

Table 5: Predicted MICs of the newly designed ligands.

Compound	MATS6c	E3p	pMIC	MIC (μg/mL)
D-1	−0.03174	0.133371	−0.01221	1.028
D-2	−0.0287	0.10996	0.138784	0.726
D-3	0.075264	0.215024	0.520779	0.301

Table 6: Binding affinities of the designed compounds and ciprofloxacin with the SipB target.

Compound	ΔG (kcal/mol)
D-1	−8.1
D-2	−7.7
D-3	−7.7
Ciprofloxacin	−7.0

D-1

D-2

D-3
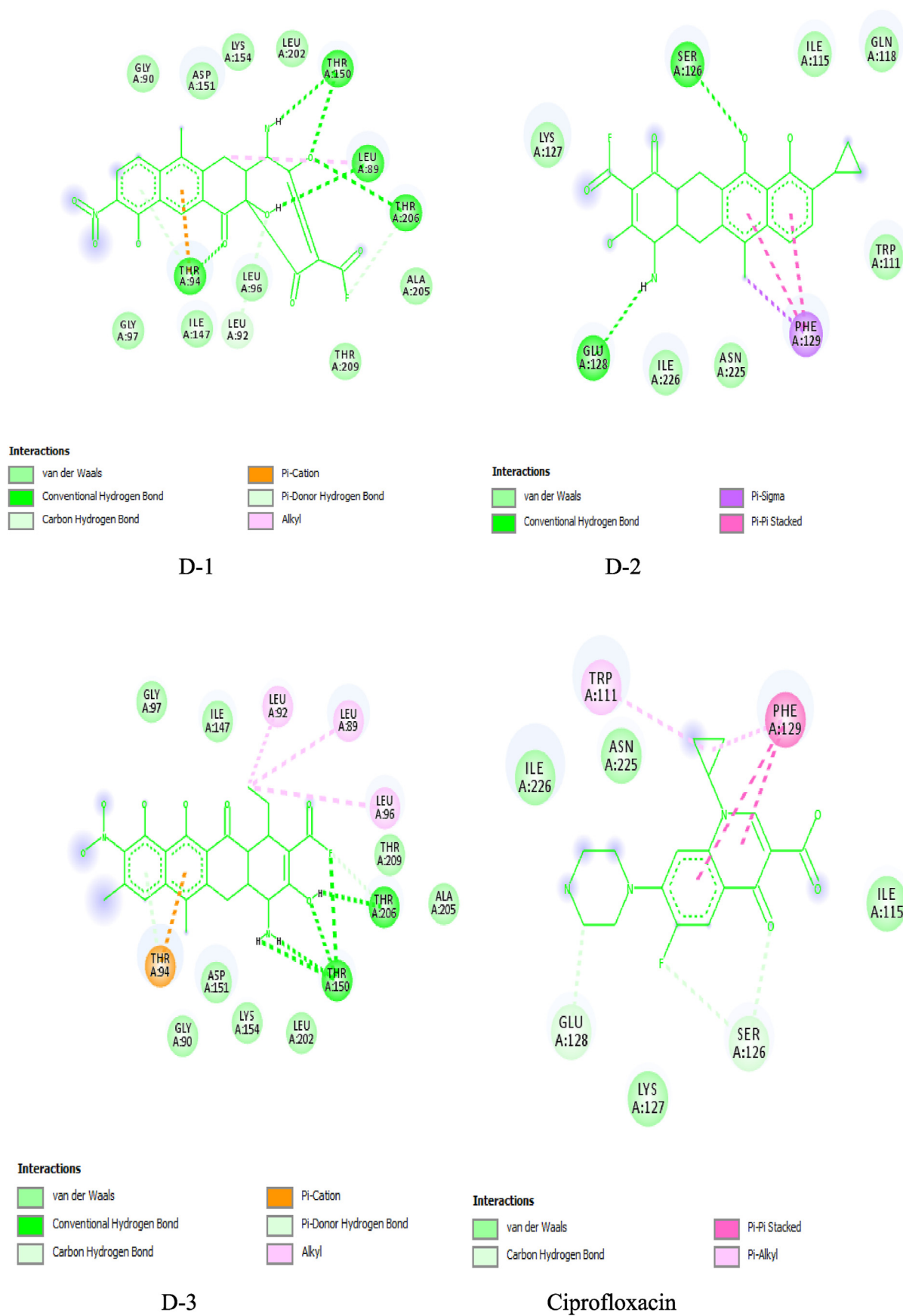
Ciprofloxacin

Figure 6: 2D interactions of the novel ligands and Ciprofloxacin with SipB target.

Table 7: Physicochemical properties and ADMET profiles of the designed ligands.

Ligand	MW (g/mol)	cLogP	cLogS	HBD	HBA	Toxicity	Pharmacokinetic
D-1	450.76	0.04	−5.10	4	10	Mutagenic: **NO** Reproductive effects: **NO** Irritant: **NO**	Solubility; **YES** CYP45 substrate; **YES** GIA: **YES** P-gp substrate: **YES**
D-2	431.85	3.10	−5.57	4	6	Mutagenic: **NO** Reproductive effects: **NO** Irritant: **NO**	Solubility; **YES** CYP45 substrate; **YES** GIA: **YES** P-gp substrate: **YES**
D-3	478.86	2.29	−6.38	4	9	Mutagenic: **NO** Reproductive effects: **NO** Irritant: **NO**	Solubility; **YES** CYP45 substrate; **YES** GIA: **YES** P-gp substrate: **YES**

GIA: gastrointestinal absorption, P-gp: P-glycoprotein.

physicochemical properties of the novel ligands presented in Table 7 show that D-1, D-2 and D-3 obey Lipinski's rule and therefore may be considered orally bioavailable.

In addition, the pharmacokinetic data for the compounds (Table 7) indicate good aqueous solubility and gastrointestinal absorption. Likewise, the compounds are substrates of P-glycoprotein (P-gp) and consequently may not have the potential to cross the blood–brain barrier. P-gp is naturally expressed on the plasma membranes of endothelial cells at the blood–brain barrier, which protects the brain from harmful substances by preventing their entry into the parenchyma from the blood circulation. The blood–brain barrier plays an important role in preventing the penetration of toxins and drugs into the central nervous system.[28]

Furthermore, drug biotransformation into inactive metabolites and subsequent excretion through the kidneys and bile are crucial considerations in the pharmacokinetic study of any drug. This function is performed predominantly by cytochrome P450 (CYP450) enzymes found largely in the liver and in lesser amounts in the small intestine, lungs, placenta and kidneys.[29] Evaluation of the pharmacokinetic and toxicity profiles of D-1, D-2 and D-3 (Table 7) revealed that all compounds are substrates of one or more CYP450 enzymes. Likewise, the toxicity data revealed that the compounds are neither mutagenic nor irritating, in addition to causing no effects on the reproductive organs.

Conclusion

To discover newer bioactive molecules in the drug development pipeline that may reverse the dangerous trend of multidrug resistance in *S. typhi*, we analyzed a data set of 32 compounds with demonstrated antibacterial activity against this pathogenic bacterium through QSAR modeling to harness the molecules' dominant structural, electronic and physicochemical features responsible for the observed biological properties. The model revealed the value of MATS6c and E3p descriptors, and indicated that the former played a major role. On the basis of these findings, we optimized several lead molecules in the data set, thus leading to the design of more potent analogues (D-1, D-2 and D-3). These novel analogues were further docked with the effector protein SipB of the bacterium and were found to show better binding specificity to the target enzyme than ciprofloxacin, a standard antibiotic used for the treatment of infections caused by *S. typhi*. In addition, drug-likeness and ADMET evaluations of the designed compounds revealed that these compounds are orally bioavailable, and exhibit excellent pharmacokinetic and toxicological profiles. These findings might be of immense benefit to the pharmaceutical industry, in facilitating faster, more cost-effective discovery and development of novel antibiotics.

Conflict of interest

The authors have no conflict of interest to declare.

Ethics approval

Not applicable

Authors' contribution

AU outlined and designed the research work. GAS and SU analyzed and supervised the study. APJ ran the computational chemistry software and drafted the manuscript. All authors have critically reviewed and approved the final draft and are responsible for the content and similarity index of the manuscript.

References

1. De Kraker MEA, Stewardson AJ, Harbarth S. Will 10 million people die a year due to antimicrobial resistance by 2050? **PLoS Med 2016**; 13:e1002184.

2. Crump JA, Luby SP, Mintz ED. The global burden of typhoid fever. **Bull World Health Organ 2004**; 82: 346−353.

3. Klemm EJ, Shakoor S, Page AJ, Qamar FN, Judge, et al. Emergence of an extensively drug-resistant Salmonella enterica serovar Typhi clone harboring a promiscuous plasmid encoding resistance to fluoroquinolones and third-generation cephalosporins. **mBio 2018**; 9: e00105−e00118.

4. Kore PP, Mutha MM, Antre VR, Oswal JR, Kshirsagar SS. Computer-aided drug design: an innovative tool for modeling. **Open J Med Chem 2012**; 2: 139−148.

5. Ameji JP, Muhammad IS, Akinleye SR, Okorn GA, Aderemi WI. Insilico predictive model for anti-microbial properties of Ni (II)-Schiff bases' complexes against *Staphylococcus aureus* and *Candida albicans*. **Int J Biochem Biophys Mol Biol 2017**; 2: 36−46. https://doi.org/10.11648/j.ijbbmb.2017 0205.11.

6. Sprous DG, Zhang J, Zhang L, Wang Z, Tepper MA. Kinase inhibitor recognition by use of a multivariable QSAR model. **J Mol Graph Model 2006**; 24(4): 278−295. https://doi.org/10.1016/j.jmgm.2005.09.004.

7. Huai Z, Yang H, Li X, Sun Z. SAMPL7 TrimerTrip host−guest binding affinities from extensive alchemical and end-point free energy calculations. **J Comput Aided Mol Des 2021**; 35(1): 117−129.

8. Ribet D, Cossart P. How bacterial pathogens colonize their hosts and invade deeper tissues. **Microb Infect 2015**; 17: 173−183. https://doi.org/10.1016/j.micinf.2015.01.004. 2015.

9. Velge P, Wiedemann A, Rosselin M, Abed N, Boumart Z, et al. Multiplicity of *Salmonella* entry mechanisms, a new paradigm for *Salmonella* pathogenesis. **Microbiologyopen 2012**; 1: 243−258. https://doi.org/10.1002/mbo3.28.

10. Rosselin M, Virlogeux-Payant I, Roy C, Bottreau E, Sizaret PY, et al. Rck of *Salmonella enterica*, subspecies enterica serovar Enteritidis, mediates zipper-like internalization. **Cell Res 2010**; 20: 647−664.

11. Zhao W, Moest T, Zhao Y, Guilhon A, Buffat C, et al. The Salmonella effector protein SifA plays a dual role in Virulence. **Sci Rep 2015**; 5: 1−10. https://doi.org/10.1038/srep12979.

12. Garai P, Gnanadhas PD, Chakravortty D. Salmonella enterica serovars Typhimurium and Typhi as model organisms Revealing paradigm of host-pathogen interactions. **Virulence 2012**; 3(4): 1−11.

13. Asakura H, Ekawa T, Sugimoto N, Momose Y, Kawamoto K, Makino S, et al. Membrane topology of *Salmonella* invasion protein SipB confers osmotolerance. **Biochem Biophys Res 2012**; 426: 654−658.

14. Chen S, Zhang C, Liao C, Li J, Yu C, Cheng X, et al. Deletion of invasion protein B in *Salmonella enterica* serovar typhimurium influences bacterial invasion and virulence. **Curr Microbiol 2015**; 71: 687−692.

15. Verma KA, Danyaya IA, Kumar A, Shuaibu SB, Hamza AU, Yahaya LN, et al. Virtual screening, molecular docking, and ADME/T analysis of natural product library against cell invasion protein SipB from *Salmonella enterica serotype typhi: in silico* analysis. **Acta Sci Pharmaceut Sci 2020**; 4(8): 20−30. https://doi.org/10.31080/ASPS.2020.04.0563.

16. Yap CW. PaDEL-descriptor: an open source software to calculate molecular descriptors and fingerprints. **J Comput Chem 2011**; 32(7): 1466−1474.

17. Kennard WR, Stone AL. Computer aided design of experiments. **Technometrics 1969**; 11(1): 137−148.

18. Rajer-Kandu K, Zupan J, Majcen N. Separation of data on the training and test set for modelling: a case study for modelling of five colour properties of a white pigment. **Chemometr Intell Lab Syst 2003**; 65(2): 221−229.

19. Ameji PJ, Awe EF, Adedirin O, Olusupo SB. Exploring structure indenture for some Schiff bases as anti-Salmonella typhi drugs: a QSAR Approach. **Int J Adv Sci Res 2016**; 2(2): 48−53. https://doi.org/10.7439/ijasr.

20. Leardi R. Genetic algorithms in feature selection. In: *Genetic algorithms in molecular modeling*. Elsevier; 1996. pp. 67−86.

21. Kunal R, Kar S, Ambure P. On a simple approach for determining applicability domain of QSAR models. **Chemometr Intell Lab Syst 2015**; 145: 22−29.

22. Noble CG, She CC, Chao AT, Shi PY. Ligand-bound structures of the dengue virus protease reveal the active conformation. **J Virol 2012**; 86: 438−446.

23. Lipinski CA. Lead and drug-likeness compounds: the rule of five revolution. **Drug Discov Today Technol 2004**; 1(4): 337−341. https://doi.org/10.1016/j.ddtec.2004.

24. Daina A, Michielin O, Zoete V. SwissADME: a free web tool to evaluate pharmacokinetics, druglikeness and medicinal chemistry friendliness of small molecules. **Sci Rep 2017**; 7:42717. https://doi.org/10.1038/srep42717.

25. Golbraikh A, Tropsha A. Beware of q2. **J Mol Graph Model 2002**; 20: 269−276.

26. Roy K, Das RN, Ambure P, Aher RB. Be aware of error measures. Further studies on validation of predictive QSAR models. **Chemometr. Intell. Lab. Syst. 2016**; 152: 18−33.

27. Jalali-Heravi M, Kyani A. Use of computer assisted methods for the modeling of the retention time of a variety of volatile organic compounds: a PCA-MLR-ANN approach. **J Chem Inf Comput Sci 2004**; 4: 1328−1335.

28. Konig F, Muller F. Transporters and drug-drug interactions: important determinants of drug disposition and effects. **Pharmacol Rev 2013**; 65: 944−966.

29. Slaughter RL, Edwards DJ. Recent advances: the cytochrome P450 enzymes. **Ann Pharmacother 1995**; 29: 619−624.